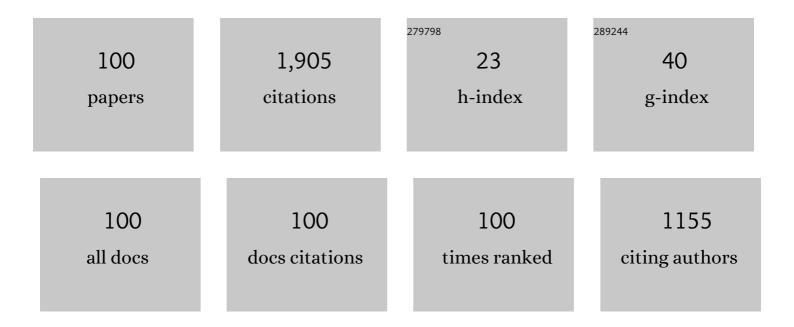
List of Publications by Year in descending order

Source: https://exaly.com/author-pdf/3155306/publications.pdf Version: 2024-02-01



#	Article	IF	CITATIONS
1	Fiber-optic bending vector sensor based on Mach–Zehnder interferometer exploiting lateral-offset and up-taper. Optics Letters, 2012, 37, 4480.	3.3	151
2	FBC-type sensor for simultaneous measurement of force (or displacement) and temperature based on bilateral cantilever beam. IEEE Photonics Technology Letters, 2001, 13, 1340-1342.	2.5	120
3	An embedded FBG sensor for simultaneous measurement of stress and temperature. IEEE Photonics Technology Letters, 2006, 18, 154-156.	2.5	100
4	Long-Period Fiber Grating Cascaded to an S Fiber Taper for Simultaneous Measurement of Temperature and Refractive Index. IEEE Photonics Technology Letters, 2013, 25, 888-891.	2.5	93
5	Two-dimensional bending vector sensing based on spatial cascaded orthogonal long period fiber. Optics Express, 2012, 20, 28557.	3.4	72
6	Bending Vector Sensor Based on a Sector-Shaped Long-Period Grating. IEEE Photonics Technology Letters, 2015, 27, 713-716.	2.5	70
7	High-Sensitivity Gas Pressure Fabry–Perot Fiber Probe With Micro-Channel Based on Vernier Effect. Journal of Lightwave Technology, 2019, 37, 3444-3451.	4.6	68
8	CO <sub>2</sub> -Laser-Induced Long Period Fiber Gratings in Few Mode Fibers. IEEE Photonics Technology Letters, 2015, 27, 145-148.	2.5	66
9	Two-dimensional microbend sensor based on long-period fiber gratings in an isosceles triangle arrangement three-core fiber. Optics Letters, 2017, 42, 4938.	3.3	53
10	Microfiber-Enabled In-line Fabry–Pérot Interferometer for High-Sensitive Force and Refractive Index Sensing. Journal of Lightwave Technology, 2014, 32, 1682-1688.	4.6	50
11	Concave-lens-like long-period fiber grating bidirectional high-sensitivity bending sensor. Optics Letters, 2017, 42, 3892.	3.3	49
12	Temperature-independent FBG-type torsion sensor based on combinatorial torsion beam. IEEE Photonics Technology Letters, 2002, 14, 1154-1156.	2.5	44
13	Bending Vector Sensor Based on a Pair of Opposite Tilted Long-Period Fiber Gratings. IEEE Photonics Technology Letters, 2017, 29, 224-227.	2.5	40
14	Bidirectional Torsion Sensor Based on a Pair of Helical Long-Period Fiber Gratings. IEEE Photonics Technology Letters, 2016, 28, 1700-1702.	2.5	37
15	2-D Medium–High Frequency Fiber Bragg Gratings Accelerometer. IEEE Sensors Journal, 2017, 17, 614-618.	4.7	36
16	Ultrasensitive Refractive Index Sensor Based on Microfiber-Assisted U-Shape Cavity. IEEE Photonics Technology Letters, 2013, 25, 1815-1818.	2.5	33
17	Two-Dimensional Bending Vector Sensor Based on the Multimode-3-Core-Multimode Fiber Structure. IEEE Photonics Technology Letters, 2017, 29, 822-825.	2.5	30
18	Ultra-high sensitivity and temperature-compensated Fabry–Perot strain sensor based on tapered FBG. Optics and Laser Technology, 2020, 124, 105997.	4.6	30

#	Article	IF	CITATIONS
19	Mach–Zehnder Interferometer Based on Interference of Selective High-Order Core Modes. IEEE Photonics Technology Letters, 2016, 28, 71-74.	2.5	28
20	Highly Sensitive In-Fiber Refractive Index Sensor Based on Down-Bitaper Seeded Up-Bitaper Pair. IEEE Photonics Technology Letters, 2012, 24, 1878-1881.	2.5	27
21	Simultaneous Force and Temperature Measurement Using S Fiber Taper in Fiber Bragg Grating. IEEE Photonics Technology Letters, 2014, 26, 309-312.	2.5	27
22	A Fiber Bending Vector Sensor Based on M-Z Interferometer Exploiting Two Hump-Shaped Tapers. IEEE Photonics Technology Letters, 2015, , 1-1.	2.5	27
23	Orthogonal Single-Polarization Single-Core Photonic Crystal Fiber for Wavelength Splitting. IEEE Photonics Technology Letters, 2012, 24, 1304-1306.	2.5	24
24	Bending Vector Sensing Based on Arch-Shaped Long-Period Fiber Grating. IEEE Sensors Journal, 2018, 18, 3125-3130.	4.7	24
25	Parallelized fiber Michelson interferometers with advanced curvature sensitivity plus abated temperature crosstalk. Optics Letters, 2020, 45, 4996.	3.3	24
26	Temperature-insensitive fiber Bragg grating force sensor via a bandwidth modulation and optical-power detection technique. Journal of Lightwave Technology, 2006, 24, 3797-3802.	4.6	23
27	Compact Long Period Fiber Grating Based on Periodic Micro-Core-Offset. IEEE Photonics Technology Letters, 2013, 25, 2111-2114.	2.5	23
28	Bending Vector Sensor Based on the Multimode-2-Core-Multimode Fiber Structure. IEEE Photonics Technology Letters, 2016, , 1-1.	2.5	23
29	Realizing torsion detection using berry phase in an angle-chirped long-period fiber grating. Optics Express, 2017, 25, 13448.	3.4	21
30	V-Shaped Long-Period Fiber Grating High-Sensitive Bending Vector Sensor. IEEE Photonics Technology Letters, 2018, 30, 1531-1534.	2.5	21
31	Ultrasensitive Fabry–Perot Strain Sensor Based on Vernier Effect and Tapered FBG-in-Hollow Silica Tube. IEEE Sensors Journal, 2021, 21, 3035-3041.	4.7	20
32	Pulse-Amplitude Equalization in a Rational Harmonic Mode-Locked Fiber Laser Using Nonlinear Modulation. IEEE Photonics Technology Letters, 2004, 16, 1813-1815.	2.5	19
33	Simultaneous Measurement of RI and Temperature Based on Compact U-Shaped Interferometer. IEEE Sensors Journal, 2020, 20, 3593-3598.	4.7	18
34	High-sensitivity bending vector sensor based on γ-shaped long-period fiber grating. Optics and Laser Technology, 2021, 142, 107255.	4.6	18
35	Beating Frequency Tunable Dual-Wavelength Erbium-Doped Fiber Laser With One Fiber Bragg Grating. IEEE Photonics Technology Letters, 2004, 16, 1453-1455.	2.5	17
36	Reconfigurable and ultra-sensitive in-line Mach-Zehnder interferometer based on the fusion of microfluid. Applied Physics Letters, 2015, 106, 084103.	3.3	17

#	Article	IF	CITATIONS
37	Torsion bidirectional sensor based on tilted-arc long-period fiber grating. Optics Express, 2019, 27, 37695.	3.4	16
38	Design of Broadband Single-Polarization Single-Mode Photonic Crystal Fiber Based on Index-Matching Coupling. IEEE Photonics Technology Letters, 2012, 24, 452-454.	2.5	15
39	Two-Octave Supercontinuum Generation of High-Order OAM Modes in Air-Core Asâ,,Sâ,ƒ Ring Fiber. IEEE Access, 2020, 8, 114135-114142.	4.2	15
40	ÂRapid Mode Decomposition of Few-Mode Fiber By Artificial Neural Network. Journal of Lightwave Technology, 2021, 39, 6294-6300.	4.6	15
41	Asymmetrically Corrugated Long-Period Gratings by Burning Fiber Coating and Etching Cladding. IEEE Photonics Technology Letters, 2013, 25, 1961-1964.	2.5	14
42	Bending vector sensor based on Mach–Zehnder interferometer using S type fibre taper and lateral-offset. Journal of Modern Optics, 2016, 63, 2146-2150.	1.3	14
43	Lab-on-tip: Protruding-shaped all-fiber plasmonic microtip probe toward in-situ chem-bio detection. Sensors and Actuators B: Chemical, 2019, 301, 127128.	7.8	13
44	Highly dispersive coupled ring-core fiber for orbital angular momentum modes. Applied Physics Letters, 2020, 117, .	3.3	13
45	Two-dimensional bending vector sensor based on Mach-Zehnder interferometer of two orthogonal lateral-offsets. Microwave and Optical Technology Letters, 2015, 57, 709-713.	1.4	12
46	Large Anomalous Dispersion at Short Wavelength and Modal Properties of a Photonic Crystal Fiber With Large Air Holes. IEEE Journal of Quantum Electronics, 2006, 42, 961-968.	1.9	11
47	Micro-Cap on 2-Core-Fiber Facet Hybrid Interferometer for Dual-Parameter Sensing. Journal of Lightwave Technology, 2019, 37, 6114-6120.	4.6	11
48	Parabolic-cylinder-like long-period fiber grating sensor based on refractive index modulation enhancement effect. Applied Optics, 2019, 58, 1772.	1.8	11
49	Simultaneous Measurement of Curvature Vector and Temperature Based on Composite Gratings Inscribed on D-Shaped Fiber. IEEE Sensors Journal, 2021, 21, 25758-25766.	4.7	11
50	Design for a Single-Polarization Photonic Crystal Fiber Wavelength Splitter Based on Hybrid-Surface Plasmon Resonance. IEEE Photonics Journal, 2014, 6, 1-9.	2.0	10
51	Helical Fiber Interferometer Using Flame-Heated Treatment for Torsion Sensing Application. IEEE Photonics Technology Letters, 2017, 29, 161-164.	2.5	10
52	Two-axis bending vector sensor based on a long-period fiber grating cascading with a hump-shaped taper. Measurement Science and Technology, 2018, 29, 095107.	2.6	10
53	Principles and realizations of FBG wavelength tuning with elastic beams. Optoelectronics Letters, 2005, 1, 5-9.	0.8	9
54	Temperature-Independent Force Sensor Based on PSLPFG Induced by Electric-Arc Discharge. IEEE Photonics Technology Letters, 2015, 27, 1946-1948.	2.5	9

#	Article	IF	CITATIONS
55	Optical screwdriving induced by the quantum spin Hall effect of surface plasmons near an interface between strongly chiral material and air. Physical Review A, 2018, 97, .	2.5	9
56	Two-dimensional microbend sensor based on the 2-core fiber with hump-shaped taper fiber structure. Optical Fiber Technology, 2019, 52, 101948.	2.7	9
57	Two-Axis Bending Sensor Based on Asymmetric Grid Long-Period Fiber Grating. IEEE Sensors Journal, 2022, 22, 10567-10575.	4.7	9
58	Method of correlation function for analyzing cross-sensitivity of strain and temperature in fiber grating sensors. Optoelectronics Letters, 2007, 3, 195-198.	0.8	8
59	Real time and simultaneous measurement of displacement and temperature using fiber loop with polymer coating and fiber Bragg grating. Review of Scientific Instruments, 2014, 85, 075002.	1.3	8
60	Torsion sensor based on two cascaded long period fiber gratings fabricated by CO2 laser pulse irradiation and HF etching technique respectively. Journal of Modern Optics, 2017, 64, 541-545.	1.3	8
61	Polarization Rotator Based on Hybrid Plasmonic Photonic Crystal Fiber. IEEE Photonics Technology Letters, 2014, 26, 2291-2294.	2.5	6
62	Temperature-Independent Micro-Refractometer Based on Cascaded In-Fiber Air Cavities With Strain-Error Correction. IEEE Sensors Journal, 2018, 18, 8773-8780.	4.7	6
63	Ultra-high sensitivity liquid level sensor based on CO2 laser local refractive index curved modulation effect. Optics and Laser Technology, 2019, 120, 105755.	4.6	6
64	Microcavity-coupled fiber Bragg grating with tunable reflection spectra and speed of light. Optics Letters, 2018, 43, 1662.	3.3	5
65	Fabrication of Dual-Wavelength Fiber Bragg Grating with a Longitudinal Stretch. Frontiers of Physics in China, 2006, 1, 108-111.	1.0	4
66	Mechanism and characteristics of asymmetrically phase-shifted corrugated long-period fiber grating fabricated by burning fiber coating and etching cladding technology. Journal of Modern Optics, 2015, 62, 584-587.	1.3	4
67	Mach–Zehnder Interferometer Based on S-Tapered All-Solid Photonic Bandgap Fiber. IEEE Photonics Technology Letters, 2015, 27, 1849-1852.	2.5	4
68	Ringing phenomenon in chaotic microcavity for high-speed ultra-sensitive sensing. Scientific Reports, 2016, 6, 38922.	3.3	4
69	Arc Radius-Chirped Long-Period Fiber Grating by High Frequency COâ,,-Laser Writing. IEEE Photonics Technology Letters, 2021, 33, 499-502.	2.5	4
70	High sensitivity optical fiber temperature sensor based on PDMS-filled with extended measuring range. Optik, 2021, 248, 168181.	2.9	4
71	Integrated Waveguide Grating Vortex Laser Generator Directly Written in Nd:YAG Crystal. IEEE Photonics Technology Letters, 2022, 34, 409-412.	2.5	4
72	Strain-tuned dual-wavelength erbium-doped fiber laser. Microwave and Optical Technology Letters, 2004, 42, 323-324.	1.4	3

#	Article	IF	CITATIONS
73	Wide wavelength-switched optical-pulse generation in an L-band mode-locked erbium-doped fiber laser. Microwave and Optical Technology Letters, 2005, 44, 196-199.	1.4	3
74	Multi-wavelength erbium-doped fiber laser based on a microstructure fiber Bragg grating. Microwave and Optical Technology Letters, 2005, 46, 162-164.	1.4	3
75	In-line polarization rotator based on the quantum-optical analogy. Optics Letters, 2016, 41, 2113.	3.3	3
76	Ultra-Compact Optical Thermo-Hygrometer Based on Bilayer Micro-Cap on Fiber Facet. IEEE Photonics Technology Letters, 2020, 32, 1089-1092.	2.5	3
77	Temperature self-compensation strain sensor based on cascaded concave-lens-like long-period fiber gratings. Applied Optics, 2020, 59, 2352.	1.8	3
78	Protruding-shaped SiO2-microtip: from fabrication innovation to microphotonic device construction. Optics Letters, 2019, 44, 3514.	3.3	3
79	Temperature compensation for micro-vibration sensor with fiber gratings. Microwave and Optical Technology Letters, 2004, 42, 474-476.	1.4	2
80	Light intensity-referred and temperature-insensitive fiber Bragg grating dynamic pressure sensor. Frontiers of Optoelectronics in China, 2008, 1, 113-118.	0.2	2
81	Controlled-Xgate with cache function for one-way quantum computation. Physical Review A, 2012, 85,	2.5	2
82	Characteristic analysis of a novel F-P interferometer based on a pair of FBGs with built-in LPFGs. Optoelectronics Letters, 2012, 8, 84-88.	0.8	2
83	A novel all-fiber micro-displacement sensor based on long period grating and tip structure. Optoelectronics Letters, 2014, 10, 176-179.	0.8	2
84	Tunable Autler–Townes Splitting in Optical Fiber. Journal of Lightwave Technology, 2019, 37, 3620-3625.	4.6	2
85	Air-Core Non-Zero Dispersion-Shifted Fiber With High-Index Ring for OAM Mode. IEEE Access, 2021, 9, 107804-107811.	4.2	2
86	High-sensitivity temperature sensor based on ethanol-sealed double helix microfiber coupler. Optical Engineering, 2020, 59, 1.	1.0	2
87	Gazing-detection of human eyes based on SVM. Optoelectronics Letters, 2005, 1, 65-68.	0.8	1
88	Improving dynamic response of a temperature-only FBG sensor. Optoelectronics Letters, 2006, 2, 101-103.	0.8	1
89	Design of supercontinuum source for coherent anti-Stokes Raman scattering microscopy. Optoelectronics Letters, 2008, 4, 103-105.	0.8	1
90	Design and fabrication of period interlaced ULPG that inhibit specific resonance peaks. Microwave and Optical Technology Letters, 2011, 53, 1470-1472.	1.4	1

#	Article	IF	CITATIONS
91	QoS routing with inaccurate information based on Hopfield neural network. , 0, , .		0
92	Invariant image encoding in neural network for target recognition. , 0, , .		0
93	A novel dual-wavelength fiber Bragg grating. Microwave and Optical Technology Letters, 2005, 44, 385-388.	1.4	0
94	A new setup to tune the center wavelength of FBGs. Optoelectronics Letters, 2005, 1, 107-109.	0.8	0
95	Applying Hopfield neural network to QoS routing in communication network. Optoelectronics Letters, 2005, 1, 217-220.	0.8	Ο
96	Illumination Variation in Images in Independent Component Analysis and Principal Component Analysis Subspaces. , 2006, , .		0
97	Reflection spectra of fiber Bragg gratings in quadratic strain field. Optoelectronics Letters, 2006, 2, 419-421.	0.8	0
98	Statistical Neural Networks Based Blind Deconvolution of Spectroscopic Data. , 2007, , .		0
99	7-Ring-Air-Core Trench-Assisted Fibre Supporting >300 Radially Fundamental OAM Modes Across S+C+L Bands. , 2021, , .		0
100	Efficient Switchable Common Path Interferometer for Transmission Matrix Characterization of Scattering Medium. IEEE Photonics Journal, 2022, 14, 1-5.	2.0	0